Available online at www.sciencedirect.com
SCIENCE DIRECT®
Physica B 373 (2006) 16–22
PHYSICA B
www.elsevier.com/locate/physb

First-principles study of structural and electronic properties of different phases of GaAs

H. Arabi[a,*], A. Pourghazi[b], F. Ahmadian[a], Z. Nourbakhsh[b]

[a]*Faculty of Science, Department of Physics, University of Birjand, Birjand, Iran*
[b]*Faculty of Science, Department of Physics, University of Isfahan, Isfahan, Iran*

Received 14 October 2005; accepted 14 October 2005

Abstract

We present a theoretical investigation of structural and electronic properties of the four known structural phases of GaAs (zinc-blende, sc16, cinnabar and Cmcm). We used the full potential linearized augmented plane wave method, within local density approximation, and also within generalized gradient approximation for the exchange correlation potential. The lattice constants, bulk modulus and its pressure derivative are calculated for each of the four phases. The data obtained for the transition pressures between different phases are presented. Band structures and densities of states of the four phases are also given. The results are compared with previous calculations and with experimental results.

PACS: 71.15.Ap; 71.15.Mb; 71.20.−b; 71.20.Nr

Keywords: Density functional theory; FP-LAPW; GaAs phases; Structural properties; Electronic properties

1. Introduction

Recently, computer simulations have made it possible to compute with great accuracy a large number of electronic and structural properties of solids from first principles. This has led to new dimensions in condensed matter studies. It is now possible to explain and to predict properties of solids under conditions, which are inaccessible to experiments [1].

GaAs is a III–V semiconductor compound, being composed of gallium (Ga) from column III and arsenic (As) from column V of the Periodic Table of the elements. GaAs in the zinc-blende structure is a direct band gap semiconductor, which makes it a very useful material for the manufacturing of light-emitting diodes and semiconductor lasers.

The structural-phase transitions in GaAS have been an area of study for a number of years. Despite this continued interest there have been some disagreements between experiment and theory on the nature and relative stability of the high-pressure phases [2]. It has been reported that increasing pressure on GaAs at 300 K will transform it from the ambient pressure zinc-blende (zb) phase to an orthorhombic structure (space group Pmm2) at 17 GPa, and then to a second orthorhombic structure (space group Imm2) at 24 GPa [3]. Recent experimental investigations show that: (I) The Pmm2 and Imm2 structures are one and the same, and the true space group for this structure is Cmcm [4], (II) On pressure decrease at 300 K, the Cmcm structure transforms to a previously unobserved hexagonal structure (cinnabar structure) before transforming back to the zb structure [5], (III) Heating the Cmcm phase to above 423 K at about 15 GPa results in transition to a second previously unobserved phase with the cubic structure (sc16), which is stable when the temperature is reduced to ambient [6].

In this paper, we investigate theoretically the structural and electronic properties of the zinc-blende, sc16, cinnabar and Cmcm phases of GaAs. This paper is organized as follows: In Section 2, we describe the computational

*Corresponding author. Tel.: +98 561 2230008; fax: +98 561 2230009.
E-mail addresses: harabi@birjand.ac.ir, arabi_h@yahoo.com (H. Arabi).

0921-4526/$ - see front matter © 2005 Elsevier B.V. All rights reserved.
doi:10.1016/j.physb.2005.10.130

approach used in the work. Structural parameters, band structure, density of states (DOS) are presented and discussed in Section 3. Finally, we present a brief conclusion.

2. Computational details

In this work, we have used the full potential linearized augmented plane wave (FPLAPW) method [7] within density functional theory (DFT). The exchange correlation potential within the local density approximation (LDA) is calculated using the scheme of Ceperley–Alder as parametrized by Perdew–Zunger [8] and within the generalized gradient approximation (GGA) using the scheme of Perdew–Burke–Ernzerhof (PBE-GGA) [9]. The computation has been carried out using the WIEN2k code [10]. In this code the unit cell is divided into no overlapping muffin-tin spheres of radius R_{MT} and an interstitial region, where the Kohn–Sham wave functions are expressed in spherical harmonics within spheres and in plane waves in the remaining space of the unit cell.

We use the value 7 for the parameter $R_{MT}K_{MAX}$ which determines the matrix size (convergence), where K_{MAX} is the cut-off wave number for the plane waves, and R_{MT} is the smallest value of all atomic-sphere radii. Basis functions, charge density, and potential were expanded inside the muffin-tin spheres in spherical harmonic functions with cut-off l_{MAX}, and in Fourier series in the interstitial region. The values of the muffin-tin radius (R_{MT}), the nearest neighbor distance, k-point number, $R_{MT}K_{MAX}$ and l_{MAX} used in this work are listed in Table 1.

3. Results and discussions

3.1. Equilibrium structural properties

The ground-state properties of high-pressure phases of GaAs were obtained using the calculations of the total energy (E_{tot}) as a function of volume (V). Fig. 1 shows the E_{tot} versus V curves for the zb, sc16, cinnabar and Cmcm phases of GaAs. These curves were obtained by calculating E_{tot} at several different volumes and by fitting the calculated values to the Murnaghan equation of state [11]. It shows that the zb phase is more stable than the other phases. The ground-state E_{tot} values of the sc16, cinnabar, and Cmcm structures are higher than that of the zb structure by 0.023, 0.03 and 0.05 eV/molecule, respectively.

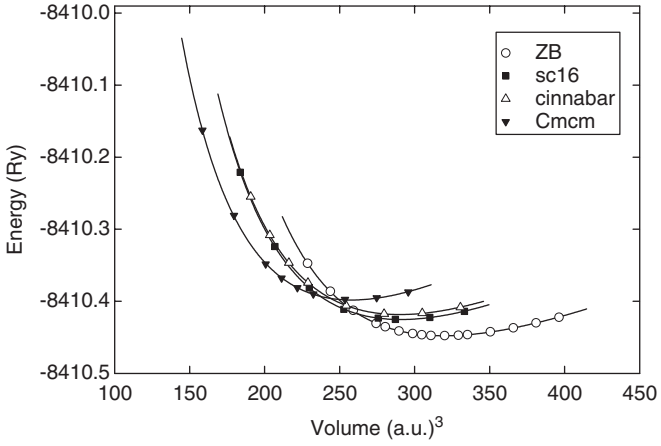

Fig. 1. Total energy versus volume curves of four phases of GaAs.

From the total energy versus volume curves, the zero-pressure equilibrium lattice constant (a_{eq}), the bulk modulus (B_0) and the pressure derivative of the bulk modulus (B') have been obtained. These results are given in Table 2, together with theoretical and experimental results of other authors.

Our calculated lattice parameters are in good agreement with the experimental and other theoretical data. In the zb phase, it is obvious that compared with the experiment, the DFT within PBE-GGA gives a higher value and within LDA gives a smaller value for the lattice parameter .The discrepancy between the calculated and measured values of the lattice parameters (with GGA) is 1.5%, 1.2%, 4.8% and 6.6% for the zb, sc16, cinnabar and Cmcm phases, respectively. The greater differences between the calculated and experimental values for the cinnabar and Cmcm phases are not unexpected, because our values have been calculated at zero pressure, while the experimental data are at 8.3 and 18.9 GPa for the cinnabar and Cmcm phases, respectively. As expected the GGA underestimates the value of the bulk modulus [12], for example in the zb phase the bulk modulus is 20% smaller than the experimental value.

Table 1
The number of k-points, the nearest-neighbor distance, $R_{MT}K_{MAX}$, l_{MAX} and the muffin-tin radius (R_{MT}) used for the zb, sc16, Cmcm and cinnabar phases of GaAs

Structure	k-points	NN(a.u.)	$R_{MT}K_{MAX}$	l_{MAX}	R_{MT}(a.u.)	
					Ga	As
zb	73	4.62571	7.00	10	2	2
sc16	119	4.46982	7.00	10	2	2
Cinnabar	274	4.48033	7.00	10	2	2
Cmcm	144	4.69997	7.00	10	2	2

3.2. Phase transformations under high pressure

The (negative value of the) gradient of the common tangent between two energy–volume curves corresponding to two different phases gives the transition pressure (p_t) between those two phases. In Table 3, the values of the transition pressures obtained are compared with the available experimental data and other theoretical results. Experimental studies suggested sc16 to be stable from 13 to 14.5 GPa [6], which is in quite good agreement with our results.

Table 2
The calculated equilibrium lattice constant, bulk modulus and its pressure derivative of zb, sc16, cinnabar and Cmcm phases of GaAs compared with other works and with experimental results

Structure	Lattice constant (Å)	B (GPa)	B'
zb			
Present work (GGA)	5.74	59.96	4.41
Present work(LDA)	5.6	72.44	4.71
Other work	5.55, 5.72 [16], 5.51, 5.79 [17]	79, 58 [16], 76, 61 [17]	
Exp.	5.653 [18]	5.65 [18]	
sc16			
Present work (GGA)	7.02	74.13	3.72
Present work (LDA)	6.85	80.99	4.09
Other work	6.546 [19], 6.871 [19]	73 [19]	4.8 [19]
Exp. (at 18.9 GPa)	6.594 [6]		
Exp. (at ambient pressure)	6.934 [6]		
Cinnabar			
Present work (GGA)	$a = 4.07$, $c = 9.08$	66.81	3.99
Present work (LDA)	$a = 3.95$, $c = 8.82$	78.44	4.27
Other work	$a = 3.883$, $c = 8.551$ [2]		
Exp. (at 8.3 GPa)	$a = 3.883$, $c = 8.657$ [5]		
Cmcm			
Present work (GGA)	$a = 5.35$, $b = 5.67$, $c = 5.13$	76.82	3.87
Present work (LDA)	$a = 5.2$, $b = 5.5$, $c = 5$	89.06	4.07
Exp. (at 18.9 GPa)	$a = 5.017$, $b = 5.325$, $c = 4.862$ [6]		

Table 3
The transition pressure between different phases of GaAs

Phase transition	Transition pressure (GPa)
zb → sc16	
Present work (GGA)	13.5
Present work (LDA)	10.35
Other work	11.5 [19]
Exp.	14.9 [20]
zb → cinnabar	
Present work (GGA)	16
Present work (LDA)	15
Other work	14.5 [21]
Exp.	Not observed
zb → Cmcm	
Present work (GGA)	14.4
Present work (LDA)	12.2
Other work	12 [23], 23.5 [22], 54 [22], 16.4 [2]
Exp.	12 [25], 12.5 [24], 17.3 [5]
sc16 → Cmcm	
Present work (GGA)	14.6
Present work (LDA)	13
Other works	12.7 [19]
Exp.	18[20]
Cmcm → cinnabar	
Present work (GGA)	10.6
Present work (LDA)	8.9
Other work	10 [20]
Exp.	11.9 [5]

The cinnabar phase of GaAs can only exist as a metastable phase. We calculate (with GGA) the coexistence pressures for Cmcm → cinnabar and zinc-blende → cinnabar at 10.9 and 16 GPa, respectively. The experimental value of the transition pressure of Cmcm → cinnabar is 11.9 GPa [5]. It is of worth to mention that the cinnabar → zinc-blende transition is not reversible from the experimental point of view. The transition pressure of zb → cinnabar is higher than the transition pressure for zb → Cmcm. If the zinc-blende → Cmcm transition was inhibited, and overcame any energy barrier between zinc-blende and cinnabar, then, the cinnabar phase would be observed upon increasing the pressure on zinc-blende phase at pressures above 16 GPa.

Compared to the other theoretical works, our calculated transition pressures in both schemes (GGA and LDA) for zb → Cmcm are in better agreement with experimental results. The transition pressure for Cmcm → cinnabar is in good agreement with the experiment. On the whole it is observed that the results by GGA are in better agreement with the experimental values than the ones by LDA.

3.3. Electronic properties

3.3.1. Band structure

The major shortcoming of the DFT theory in calculating energy gaps lies in the exchange correlation term, which cannot be calculated accurately within this method. GGA improves the results compared to LDA, but the exchange correlation energy and its charge derivative cannot be obtained accurately. This is due to the fact that GGA has a simple form and is not sufficiently flexible to accurately reproduce both of them [13].

Considering this shortcoming, Engel and Vosko [14] constructed a new functional form of GGA (abbreviated as EV-GGA) to calculate exchange correlation potential.

Dufek et al. [15] have applied EV-GGA to a wide range of solids and have compared the results with other GGA-based calculations. They concluded that EV-GGA improves the determination of the band gap and of some other properties. Results based on total-energy calculations, such as equilibrium lattice parameters and bulk modulus with EV-GGA show a large difference with experimental values.

We have calculated the band structures of the four phases of GaAs along some high symmetry directions in the first Brillouin zone using LDA, PBE-GGA and also EV-GGA. The band structures show that the zb, cinnabar and sc16 phases are semiconducting and that the Cmcm phase is metallic. The band gaps, displayed in Table 4, were calculated using LDA, PBE-GGA and EV-GGA. The experimental and other theoretical calculations are given as well.

The important features to note for each phase are explained as follows:

(a) *The zinc-blende phase*: The band structure of the zb phase is shown in Fig. 2. The direct energy gap is at the Γ point between the top of the As p valence band and a mixture of predominantly Ga s as well as As s bands which is at the bottom of the conduction band at Γ. The direct band gap obtained by the EV-GGA method is 1.1 eV which is in good agreement with the experimental band gap. Although the band gap calculated with PBE-GGA is closer to the experimental value than the one obtained with LDA, both schemes underestimate the band gap. The width of the upper valence band is 6.836 eV and the width of the lower valence band is 2.566 eV.

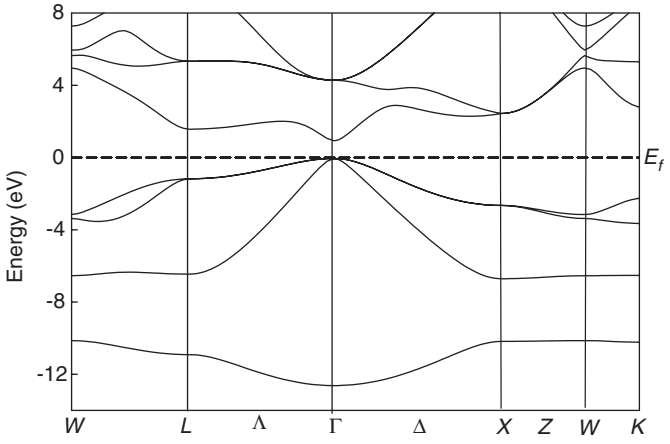

Fig. 2. Band structure of the zb phase of GaAs, calculated by EV-GGA.

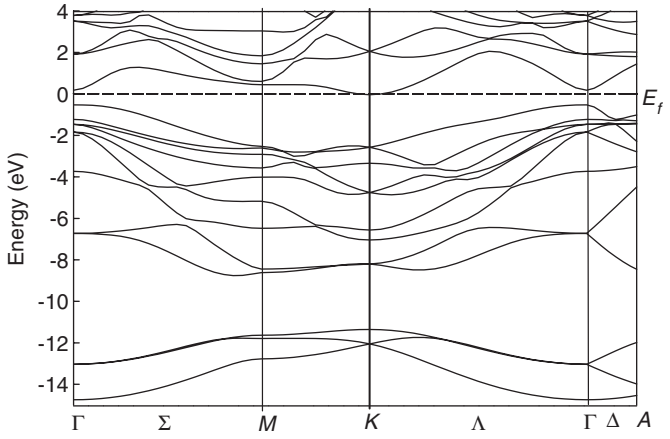

Fig. 3. Band structure of the cinnabar phase of GaAs at 16 GPa calculated by EV-GGA.

Table 4
Calculated energy gap (E_g) for semiconducting phases of GaAs

Structure		E_g (eV)
Zb		
Present work (LDA)	$(\Gamma-\Gamma)$	0.28
Present work (GGA-PBE)	$(\Gamma-\Gamma)$	0.51
Present work (GGA-EV)	$(\Gamma-\Gamma)$	1.1
Other works (GGA)	$(\Gamma-\Gamma)$	1.08 [16]
Other works (LDA)	$(\Gamma-\Gamma)$	0.92 [16]
Exp. (at 300 K)	$(\Gamma-\Gamma)$	1.41 [18]
Cinnabar		
In the equilibrium structure		
Present work (LDA) (at 15 GPa)	$(K-\Gamma,K)$	−0.11
Present work (GGA-PBE)(at 16 GPa)	$(K-\Gamma,K)$	−0.076
Present work (GGA-EV)(at 16 GPa)	$(K-\Gamma,K)$	0.337
Other work (at 16 GPa)	$(\Gamma-M)$	0.26 [2]
At zero pressure		
Present work (GGA-EV)	$(K-\Gamma,K-\Gamma)$	0.017
Other work	$(\Gamma-\Gamma)$	0.09 [2]
sc16		
In the equilibrium structure		
Present work (LDA) (at 10.35 GPa)	$(\Gamma-\Gamma)$	0
Present work (GGA-PBE) (at 13.5 GPa)	$(\Gamma-\Gamma)$	0
Present work (GGA-EV) (at 13.5 GPa)	$(\Gamma-\Gamma)$	0
At zero pressure		
Present work (GGA-EV)	$(\Gamma-\Gamma)$	0

(b) *The cinnabar phase*: We have also investigated the electronic structure of the cinnabar phase. We calculated, by the EV-GGA method, the band structure for the equlibrium structure, which is shown in Fig. 3. It is found that the cinnabar phase is semiconducting with an indirect band gap between the K point in the conduction band and along $\Gamma-K$ of the valence band of 0.337 eV at 16 GPa.Our result is in reasonsable agreement with other results. The values obtained by PBE-GGA and LDA are negative. The unstable zero-pressure cinnabar structure is also semiconducting with an indirect band gap of 0.017 eV. In the equlibrium structure, the width of the upper valence band is 8.165 eV and that of the lower valence bandwidth is 3.382 eV.

(c) *The sc16 phase*: The band structure of the sc16 phase is shown in Fig. 4, which has been calculated by EV-GGA. There is a direct band gap at the Γ point of 0 eV.The width of the upper valence band is 7.98 eV and of the lower valence band is 3.164 eV. The band gaps calculated by

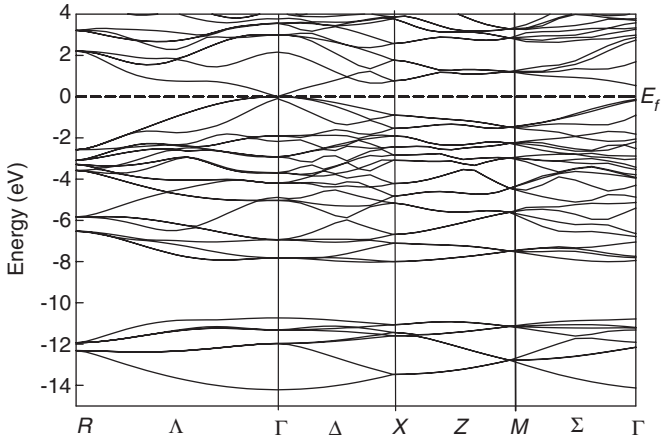

Fig. 4. Band structure of the sc16 phase of GaAs at 13.5 GPa calculated by EV-GGA.

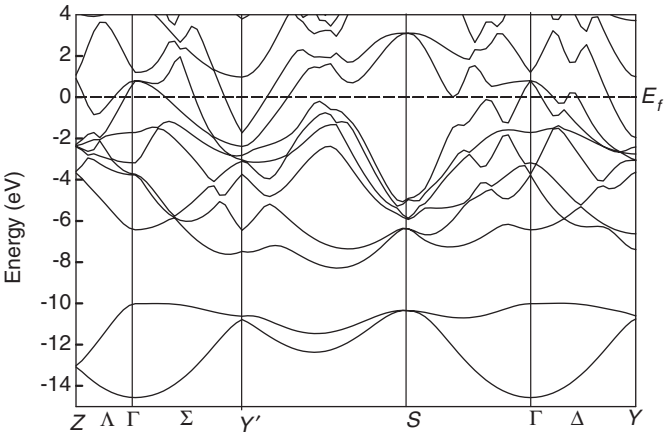

Fig. 5. Band structure of the Cmcm phase of GaAs.

PBE-GGA and LDA have the same values as the ones obtained with EV-GGA. Furthermore, the sc16 structure is at the border between semiconducting and metallic. To our knowledge no electronic structure calculation has been reported for this phase in the literature.

(d) *The Cmcm phase*: The band structure of the Cmcm phase of GaAs was calculated using the experimental values of the lattice constants at 20 GPa. It is shown in Fig. 5 that this phase is metallic because the energy bands cross the Fermi level.

The general results to note for all band structures are as follows:

1. The occupied bands for all phases are separated into two sub-bands with gaps of 3.346, 2.59 and 2.696 eV for zb, cinnabar and sc16, respectively.
2. The values of the band gaps of the semiconducting phases calculated using EV-GGA are in reasonable agreement with the other results.
3. The band gap (valence-conduction) is decreasing from zb to sc16 phase.
4. It seems that, for all semiconducting phases LDA and PBE-GGA underestimate the band gap while EV-GGA overstimates it.

3.3.2. Density of states

3.3.2.1. The zinc-blende phase. The total and partial DOS of the zb phase of GaAs have been calculated by means of the tetrahedral method [26]. The total DOS of the zb phase of GaAs is shown in Fig. 6(a), while the contribution of Ga and As are shown in Figs. 6(b) and 6(e), respectively. The partial DOS of the s and p orbitals of Ga and As are presented in Fig. 6 in parts (d), (c), and (g), (f), respectively.

The positions of the peaks are in reasonable agreement with earlier calculations. It is further observed that the first peak encountered in the total DOS for GaAs in Fig. 6(a) is small but relatively broad, centered around −11 eV. It is seen from the partial DOS for As that the peak arises almost entirely from As 4s states (Fig. 6(g)). This peak corresponds to the lowest lying band in Fig. 2, with its width arising from the dispersion in the region around the Γ point in the Brillouin Zone.

The peak at −6.25 eV corresponds to the Ga 4s states (Fig. 6(d)) that are mixed with the As 4p states (Fig. 6(f)).

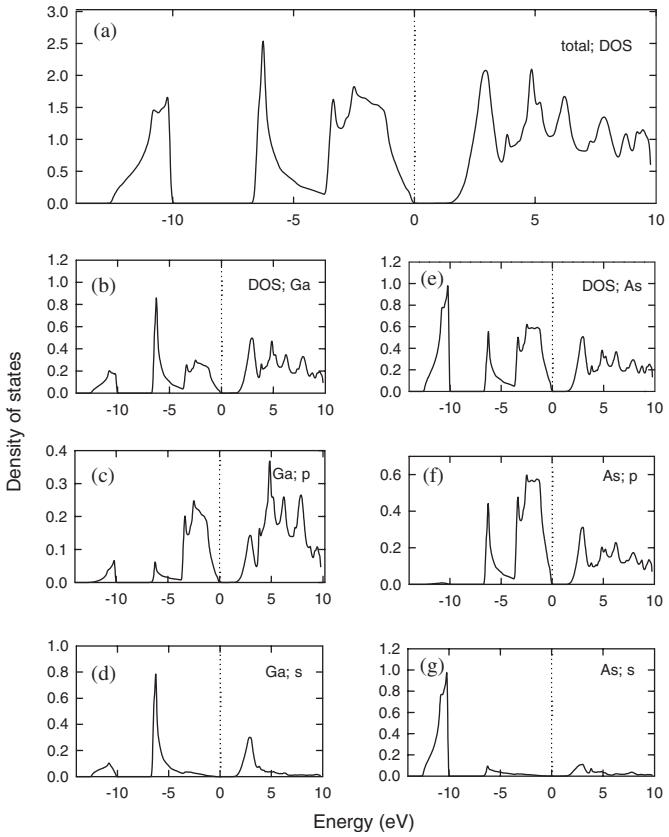

Fig. 6. Total and partial DOS of the zinc-blende phase of GaAs: (a) total DOS, (b) and (e) partial DOS of Ga and As. The partial DOS of the s and p orbitals of Ga and As are shown in parts of (d), (c), and (g), (f), respectively.

The hump between −3.7 eV and zero energy corresponds to the As 4p states (Fig. 6(f)) that are mixed with the Ga 4p states (Fig. 6(c)). The peak at 2.91 eV (above the Fermi level) is due to equal contributions of the Ga 4s and As 4p states (Fig. 6(d) and (f)).

On the whole, it is seen that below and close to the Fermi level, the As 4p states dominate, wheras above and close to Fermi level Ga 4s and As 4p states dominate. It is also of worth to say that the DOS of the cinnabar and sc16 phases are rather similar to that of the zb phase.

3.3.2.2. The Cmcm phase. The DOS of the Cmcm phase of GaAs is shown in Fig. 7. The total DOS is shown in Fig. 6(a), while the total DOS of Ga and As are shown in Figs. 6(b) and (f), respectively. The partial DOS of the s, p and d orbitals of Ga and As are presented in Fig. 6 in parts (e), (d), (c) and (i), (h), (g), respectively.

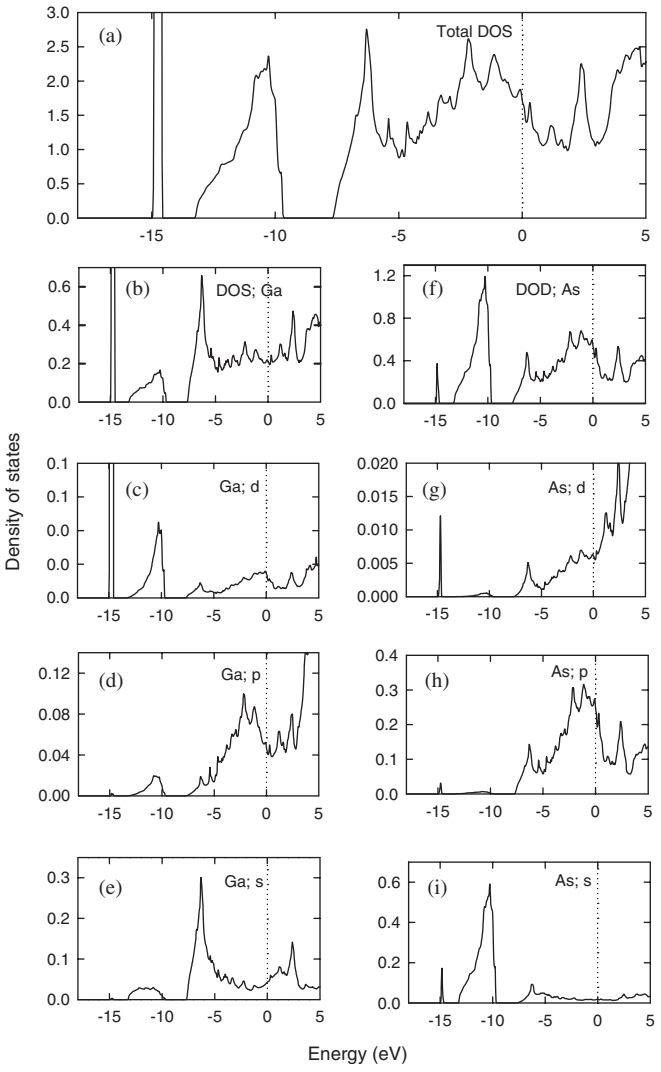

Fig. 7. Total and partial DOS of the Cmcm phase of GaAs: (a) total DOS of GaAs. (b) and (f) partial DOS of Ga and As. The paritial DOS of the s, p and d orbitals of Ga and As are shown (e), (d), (c) and (i), (h), (g), respectively.

The sharp peak in the total DOS in the energy between −14.99 and −14.55 eV (Fig. 7(a)) arises from Ga 3d states (Fig. 7(c)). The electronic states between −13.27 and −9.66 eV are due to As 3s (Fig. 7(i)), with a maximum peak value at −10.28 eV. The DOS between −7 and −5 eV consists of Ga 3s, As 3s and As 3p (Figs. 7(e), (I) and (h)). The peak in this region occurs at −6.3 eV and the major contribution to this peak is due to Ga 3 s (Fig. 7(e)). In the interval from −5 eV to zero energy the major contribution to the total DOS comes from As 3p with a small admixture of Ga 3p states (Fig. 7(h) and (d)). Finally, the DOS above the Fermi level is mainly due to Ga 3 s, Ga 3p and As 3p states (see Figs. 7(e), (d) and (h)).

4. Conclusions

In this paper, using the FPLAPW method, we have presented a complete analysis of the structural and electronic properties of four phases of GaAs.

We conclude that the use of PBE-GGA for the exchange correlation potential permitted us to obtain good structural parameters, but that this approximation is not appropriate for calculating the band gaps. By using the GGA of Engel and Vosko, we performed band structure calculations and obtained reasonable values for the band gaps.

We also calculated the transition pressures between different phases and conclude that our results with PBE-GGA are very close to the experimental results.

Finally, the total and partial DOS were obtained.

Acknowledgments

Hadi Arabi, would like to thank the magnetic materials group of the Van der Waals–Zeeman Institute, University of Amsterdam, Amsterdam (The Nederlands), where he performed this work in part, for its hospitality.

References

[1] R. Khenata, H. Baltache, M. Sahnoun, M. Driz, M. Rerat, B. Abbar, Physica B 336 (2003) 321.
[2] A.A. Kelsey, G.J. Ackland, S.J. Clark, Phys. Rev. B 57 (1998) R2029.
[3] S.T. Weir, Y.K. Vohra, C.A. Vanderborgh, A.L. Ruoff, Phys. Rev. B 39 (1989) 1280.
[4] M.I. McMahon, R.J. Nelmes, Phys. Stat. Sol. (b) 198 (1996) 389.
[5] M.I. McMahon, R.J. Nelmes, Phys. Rev. Lett. 78 (1997) 3697.
[6] M.I. McMahon, R.J. Nelmes, D.R. Allan, S.A. Belmonte, T. Bovornratanaraks, Phys. Rev. Lett. 80 (1998) 5564.
[7] J.C. Slater, Adv. Quant. Chem. 1 (1994) 35.
[8] J.P. Perdew, A. Zunger, Phys. Rev. B 23 (1981) 5048.
[9] J.P. Perdew, S. Burke, M. Ernzerhof, Phys. Rev. Lett. 77 (1996) 3865.
[10] P. Blaha, K. Schwarz, G.K.H. Madsen, D. Kvasnicka, J. Luitz, WIEN2K, An Augmented Plane Wave + Local Orbitals Program for Calculating Crystal Properties, Karlheinz Schwarz, Technical Universität, Wien, Austria, ISBN 3-9501031-1-2, 2001.
[11] F.D. Murnaghan, Proc. Natl. Acad. Sci. USA 30 (1994) 244.
[12] C. Filippi, D.J. Singh, C.J. Umrigar, Phys. Rev. B 50 (1994) 14947.
[13] A. Mokhtari, H. Akbarzadeh, Physica B 337 (2003) 122.
[14] E. Engel, S.H. Vosko, Phys. Rev. B 47 (1993) 13164.
[15] P. Dufek, P. Blaha, K. Schwarz, Phys. Rev. B 50 (1994) 7279.

[16] R. Miotto, G.P. Srivastava, Phys. Rev. B 59 (1999) 3008.
[17] A. DalCorso, A. Pasquarello, A. Baldereschi, R. Car, Phys. Rev. B 53 (1996) 1180.
[18] O. Madelung (Ed.), Semiconductors, Group IV Elements and III–V Compounds, Landolt–Bornstein, New Series, Group III, vol. 17, Pt. a, Springer, Berlin, 1991.
[19] A. Mujica, R.J. Needs, A. Munoz, Phys. Rev. B 52 (1995) 8881.
[20] M.I. McMahon, T. Bovornratanaraks, D.R. Allan, S.A. Belmonte, The University of Edinburgh, Edinburgh, Lothian EH9 3JZ, UK.; Y. Wang, T. Uchida, M. Rivers, S. Sutton, CARS-CAT, Advanced Photon Source, Argonne National Laboratory, Argonne, IL 60439, USA
[21] A. Mujica, A. Munoz, Phys. Rev. B 57 (1998) 1344.
[22] M. Durandurdu, D.A. Drabold, Phys. Rev. B 66 (2002) 045209.
[23] A. Mujica, R.J. Needs, J. Phys: Condens. Matter 8 (1996) L237.
[24] Y.G. Gogotsi, V. Domnich, S.N. Dub, A. Kailer, K.G. Nickel, J. Mater. Res. 15 (4) (2000) 871.
[25] J.M. Besson, J.P. Itie, G. Wiell, J.L. Mansot, J. Ganzalez, Phys. Rev. B 44 (1991) 4214.
[26] P.E. Blochl, O. Jepsen, O.K. Anderson, Phys. Rev. B 49 (1994) 1623.